Fabrication and Characterization of Single Pores for Modeling Mass Transport across Porous Membranes

Li Sun* and Richard M. Crooks

Department of Chemistry, Texas A&M University, P.O. Box 30012, College Station, Texas 77842

Received July 13, 1998. In Final Form: December 2, 1998

An Au membrane containing a single pore was fabricated using a template approach. The pore diameter is defined by the diameter of a glass fiber template and the pore length by the amount of Au electroplated over a seed pore. The utility of the single pore for modeling mass transport is demonstrated by configuring the pore as a Coulter counter to monitor the transport of 440 nm diameter polystyrene spheres. An important advantage of this Au membrane model is that the pore surface chemistry can be modified with a self-assembled monolayer. However, the metallic Au surface also requires minimizing the exposed membrane area in order to reduce the interfering charging/faradaic current and to shorten the instrumental response time.

Introduction

Mass transport, particularly molecular transport, in nanoporous media is of interest to chemists for many technologically important reasons: including zeolite-based catalysis, separation using various forms of chromatography, chemical detection in porous matrixes, and cellular activity of membrane proteins.[1−4] To gain a fundamental understanding of mass transport kinetics, we are beginning to build membrane models that contain only a single nanopore. Initially, we wish to exam the effects of three structural parameters on the rate of transport: namely, the diameter, the length, and the surface chemistry of the pore (Scheme 1).

Two major types of model membranes have been used in previous studies. The first type contains an array of pores with polydispersed pore diameter, pore length, and surface sites.[5−7] Quantitative analysis of the data obtained from such a model is complicated although qualitative insights about transport mechanisms can be obtained.[8−10] The second type of model membrane contains pores with one or more monodispersed structural parameters.[11−17]

Scheme 1

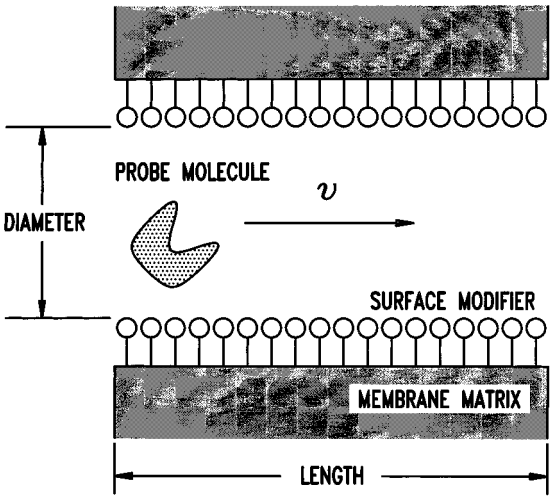

This model permits a more direct and quantitative correlation between the membrane structure and the transport rate because all pores behave identically. However, under steady state conditions, only an averaged transport rate can be determined because particles being transported do not enter membrane pores at the same time so that the measured signal is a spatially and temporally averaged one. In addition, it is increasingly difficult to ensure structural uniformity as the pore dimensions decrease. Sometimes only one structural parameter can be kept uniform. For example, the pore diameter of a track-etched polycarbonate membrane is uniform but the pore length varies slightly because of the dispersion in the track tilt angle.[18]

In contrast, the single-pore model presented here allows examination of individual stochastic transport

* To whom correspondence should be addressed.

(1) Buttersack, C.; Rudolph, H.; Mahrholz, J.; Buchholz, K. *Langmuir* **1996**, *12*, 3101−3106.
(2) Giddings, J. C. *Unified Separation Science*; Wiley: New York, 1991.
(3) Hoyt, A. E.; Ricco, A. J.; Yang, H. C.; Crooks, R. M. *J. Am. Chem. Soc.* **1995**, *117*, 8672−8673.
(4) Bustamante, J. O.; Liepins, A.; Hanover, J. A. *Mol. Membr. Biol.* **1994**, *11*, 141−150.
(5) Wen, L.; Li, M.; Schlenoff, J. B. *J. Am. Chem. Soc.* **1997**, *119*, 7726−7733.
(6) Shea, K. J.; Stoddard, G. J.; Shavelle, D. M.; Wakui, F.; Choate, R. M. *Macromolecules* **1990**, *23*, 4497−4507.
(7) *Perfluorinated Ionomer Membranes*; Eisenberg, A., Yeager, H. L., Eds.; ACS Sym. Ser. 180; American Chemical Society: Washington, DC, 1982.
(8) De Vidts, P.; White, R. E. *J. Electrochem. Soc.* **1997**, *144*, 1343−1353.
(9) Wang, X.-L.; Tsuru, T.; Nakao, S.-I.; Kimura, S. *J. Membr. Sci.* **1995**, *103*, 117−133.
(10) Davis, H. T.; Valencourt, L. R.; Johnson, C. E. *J. Am. Ceram. Soc.* **1975**, *58*, 446−452.
(11) Conner, M. D.; Janout, V.; Kudelda, I.; Dedek, P.; Zhu, J.; Regen, S. L. *Langmuir* **1993**, *9*, 2389−2397.
(12) Nishizawa, M.; Menon, V. P.; Martin, C. R. *Science* **1995**, *268*, 700−702.
(13) Hulteen, J. C.; Jirage, K. B.; Martin, C. R. *J. Am. Chem. Soc.* **1998**, *120*, 6603−6604.
(14) Masuda, H.; Fukuda, K. *Science* **1995**, *268*, 1466−1468.
(15) Fang, Y.; Leddy, J. *J. Phys. Chem.* **1995**, *99*, 6004−6073.
(16) Miller, C. J.; Widrig, C. A.; Charych, D. H.; Majda, M. *J. Phys. Chem.* **1988**, *92*, 1928−1936.
(17) Kemery, P. J.; Steehler, J. K.; Bohn, P. W. *Langmuir* **1998**, *14*, 2884−2889.
(18) Schönenberger, C.; van der Zande, B. M. I.; Fokkink, L. G. J.; Henny, M.; Schmid, C.; Krüger, M.; Bachtold, A.; Huber, R.; Birk, H.; Staufer, U. *J. Phys. Chem.* **1997**, *101*, 5497−5505.

10.1021/la980871a CCC: $18.00
Published on Web 01/08/1999

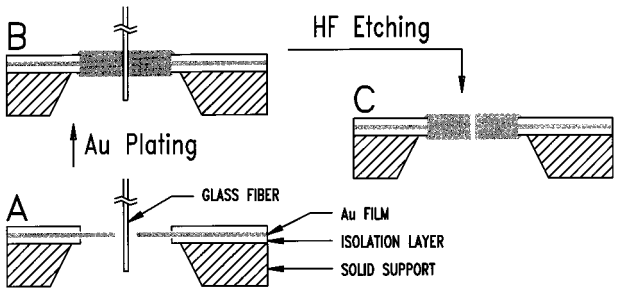

Figure 1. Schematic illustration of a template method for fabricating single pore membranes: (A) insertion of a glass template fiber into a seed pore across a free-standing Au membrane; (B) controlled deposition of an Au layer via electroplating, resulting in simultaneous diameter reduction and length elongation of the seed pore; (C) chemical removal of the template fiber with concentrated HF (48%).

events. This will provide us with additional information unattainable with an array-pore model: for example, the statistical distribution of the transport rate as well as any gating response similar to that shown by an ion channel protein. Several recent reports have illustrated the use of single-pore models for studying mass transport at the most fundamental level.[19] Another important reason for us to adopt the single-pore model is related to our interest in developing a Coulter molecular counter for mass-transport studies. A Coulter counter requires the use of a single pore whose diameter must be comparable to the size of the object being transported.[20] A single transport event is recorded as a current or voltage pulse, and the duration of the pulse is a direct measure of the transport rate. The single pore reported here is still too large for detecting single molecules, but the pore is adequate for counting polystyrene particles and represents a first step toward our ultimate objective. It should be pointed out, however, that a single-pore model is often more difficult to fabricate and requires more sensitive analytical techniques for transport measurements than an array-pore model.

Experimental Section

Solvents. Water of 18.2 MΩ cm resistivity (Milli-Q, Millipore) was used in all electrochemical measurements, and distilled water was used in all photolithographic processing steps. Absolute ethanol (Quantum Chemical, Tuscola, IL) was used as received.

Fabrication of Single Nanopores across Au Membranes (Figure 1). Microscope cover slides (12 mm diameter and #2 thickness: Erie Scientific, Portsmouth, NH) were placed in a Teflon holder and cleaned by immersion in a 2% MICRO cleaner solution (Baxter International) for over 24 h. The slides were rinsed with copious amounts of water and then with absolute ethanol, followed by drying under a flowing N_2 stream. A pinhole-free Au film (400 nm mass thickness) was deposited on the slides at a 2−5 Å/s rate in a thermal evaporator (TFS Technologies, Albuquerque, NM) of 5×10^{-6} Torr base pressure. The slide-supported Au film was transferred and glued with Apiezon W wax (M&I Material, Manchester, England) to a Si(100) support wafer containing a 1 mm by 1 mm opening. The opening was micromachined in a clean room[21] according to a literature procedure (Si_3N_4 as the etch stop and 30% KOH at 90 °C as the etchant).[22] Dissolution of the glass slide in concentrated HF (48%, EM Science) resulted in a free-standing Au membrane of about 1 mm^2 area that was draped over the square opening.

A 4 μm diameter circular patch of the Au membrane was further isolated via photolithography (AZ P4210 photoresist, Clariant, Somerville, NJ) using a home-built apparatus (mainly a modified Nikon Diaphot 300 microscope). After the patch was electrochemically removed at 0.7 V (vs an Au wire) in a two-electrode cell containing 0.1 M KCN and 0.1 M pH 12 phosphate buffer,[23] a seed pore of about 5 μm diameter was obtained (Figure 1A). The resist layer was then stripped with ethanol.

Straight fibers of 0.5−2 μm diameter were removed from a glass fiber filter (S61631, Gelman Sciences) with a pair of tweezers. One single fiber of a suitable diameter among a fiber bundle was identified under a 30× stereo-microscope and glued to a 0.010 in. diameter W wire (Johnson and Matthey) precoated with AZ P4210 photoresist. After the resist was heat-cured, the fiber was pulled out completely from the bundle.

Immediately after being ozone cleaned for 30 min (model 13550 ozone cleaner, Boekel, Feasterville, PA), the Au sample containing the seed pore was positioned inside an empty beaker. Manipulated through the W wire with a xyz stage (model 462, Newport, Irvine, CA), the glass fiber (ozone cleaned for 10 min) was inserted into the seed pore (Figure 1A). An Au electroplating solution containing 40 mM $KAu(CN)_2$, 0.5 M KH_2PO_4, and 0.25 M potassium citrate (all from Johnson and Matthey) was then poured into the beaker. Au was deposited galvanostatically at 0.2 mA/cm^2 (about 12 nm/min if the cathodic efficiency is 100%) using a Pt counter electrode.[23] After a desired thickness was reached, the Au plating solution was removed, and the sample was carefully rinsed with several drops of water (Figure 1B). The glass fiber was released from the W wire by wetting the sample with a small HF drop. Further etching in HF (48%) for 12 h dissolved the glass fiber inside the pore (Figure 1C).

Optical Microscopy. Samples were examined routinely throughout their fabrication under an optical microscope equipped with a camera port (Optiphot, Nikon). Measurements of a pore diameter from an image on the CCD TV monitor or from a digitized optical micrograph were calibrated with the image of a standard sample (1.0 or 10 μm pitch grids, Digital Instruments, Santa Barbara, CA). The measurement uncertainty was about ±0.3 μm.

Electrochemical Measurements. The Au membrane sample was clamped between two cells made of PEEK plastics.[24] The sample-to-cell surfaces were sealed with two silicone O-rings (size 2-010, Parker, Cleveland, OH). Each cell was fitted with a homemade Ag/AgCl electrode and was filled with 9 mL of solution containing 0.1 M KCl (EM Science) and 0.2 mg/mL Triton X-100 (Sigma Chemical). In some experiments, the solution in one cell was dosed with polystyrene spheres (440 nm COOH-terminated, Bangs Labs, Carmel, IN). Current and potential across a membrane were measured with an amplifier interfaced to a PC computer (Axopatch 200B and Digipack 1200, Axon Instruments, Foster City, CA). The linear potential sweep for cyclic voltammetry was generated with a universal programmer (model 175, EG&G PAR, Princeton, NJ).

Results and Discussion

Figure 2 shows optical micrographs of a single pore fabricated according to the above template method. Although measuring the pore diameter is straightforward, the inner pore surface cannot be imaged easily. One might speculate that the pore surface is as rough as the surface beyond the rim of the pore (Figure 2A);[25] however, we think that the roughness is defined primarily by the fiber surface. Since a very slow electroplating rate is used, the film growth is far from the diffusion-controlled regime. It

(19) A few related studies include: Bath, B. D.; Lee, R. D.; White, H. S.; Scott, E. R. *Anal. Chem.* **1998**, *70*, 1047−1058. Wei, C.; Bard, A. J.; Feldberg, S. W. *Anal. Chem.* **1997**, *69*, 4627−4633. Kobayashi, Y.; Martin, C. R. *J. Electroanal. Chem.* **1997**, *431*, 29−33. Vishnyakov, A.; Piotrovskaya, E. M.; Brodskaya, E. N. *Langmuir* **1996**, *12*, 3643−3649.

(20) Lines, R. W. In *Particle Size Analysis*; Stanley-Wood, N. G., Lines, R. W., Eds.; Royal Society of Chemistry: Cambridge, 1992.

(21) Microtechnology Laboratory (MTL), University of Minnesota.

(22) Stoller, A. I. *RCA Rev.* **1970**, 271−275.

(23) Electrochemical etching or plating were controlled with a PINE potentiostat (model AFRDE5, PINE Instrument, Grove City, PA).

(24) At this point, the Au surface may be modified with a SAM; however, this work only involves bare Au surface which is covered later by specifically adsorbed Cl^- ions.

(25) The RMS (root-mean-square) roughness obtained from a STM image of the membrane surface is about 93 nm.

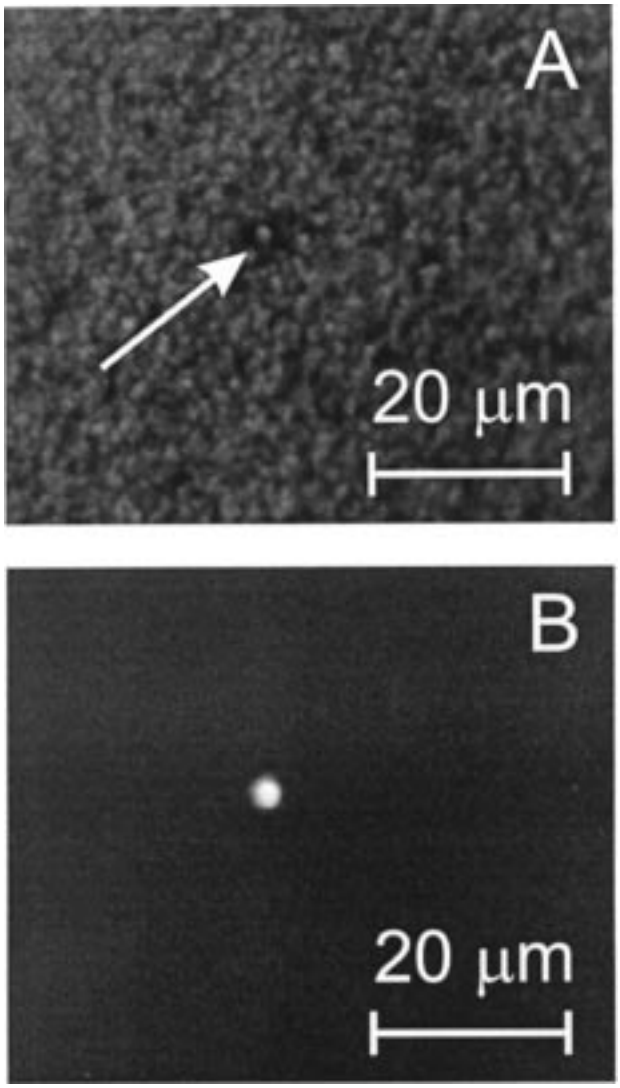

Figure 2. Optical micrographs of a single-pore membrane under (A) front and back illumination and (B) back illumination only. The arrow in A points to the pore which is barely visible because of the rough surface surrounding the pore.

is unlikely that any void space is trapped between the fiber surface and the pore surface.

The fiber template is an important feature of our method for pore fabrication. Using the fiber ensures effective control over both pore diameter and pore length. From Figure 1, one can see that the pore diameter is equal to the fiber diameter while the pore length is about twice the thickness of the electroplated Au (plus the seed membrane thickness). One problem of the present method is that it requires too many fabrication steps, which leads to a long fabrication time and a low device yield.

There exists a close correlation between the structural parameters of a nanopore (pore diameter, length, and surface chemistry) and its performance characteristics as a Coulter counter. The observed membrane current, i_m, across a single metallic pore can be written as

$$i_m = i_c + i_f + i_p \qquad (1)$$

where i_c is the capacitive charging current and i_f is the faradaic current across the membrane/electrolyte interface. i_c is observable only when the membrane potential, E_m, changes. Charge neutrality requires that i_f corresponds to a cathodic reaction at one side of the membrane while an equal magnitude of anodic current passes through the other side of the membrane. The ionic current across the pore itself, i_p, is given by eq 2[26]

$$i_p = \frac{E_m}{R_p} = \frac{\kappa \pi d^2 E_m}{4l} \qquad (2)$$

where R_p is the pore resistance, κ is the electrolyte conductivity, d is the effective pore diameter, and l is the pore length. i_p will change when R_p changes, e.g., when a particle moves into the pore, causing a decrease in the effective pore diameter d. Equation 2 ignores the "end effect", which introduces a significant error when the l/d ratio approaches 1.[27] The end effect originates from the ion flux extending outside the pore entrance or exit.

It is desirable to minimize i_c and i_f: i.e., the capacitive and faradaic (CF) current since only a change in i_p carries analytical information in a Coulter counter. Figure 3 shows the relative magnitude of the three current components. Without a pore, only the CF current is visible (Figure 3A): the rectangular loop is characteristic of a capacitor while the slight tilt is caused either by the electrolysis of trace redox impurities or by an unknown leakage pathway across the metallic membrane.[28] To reduce the CF current, the area of the exposed Au surface near the pore is

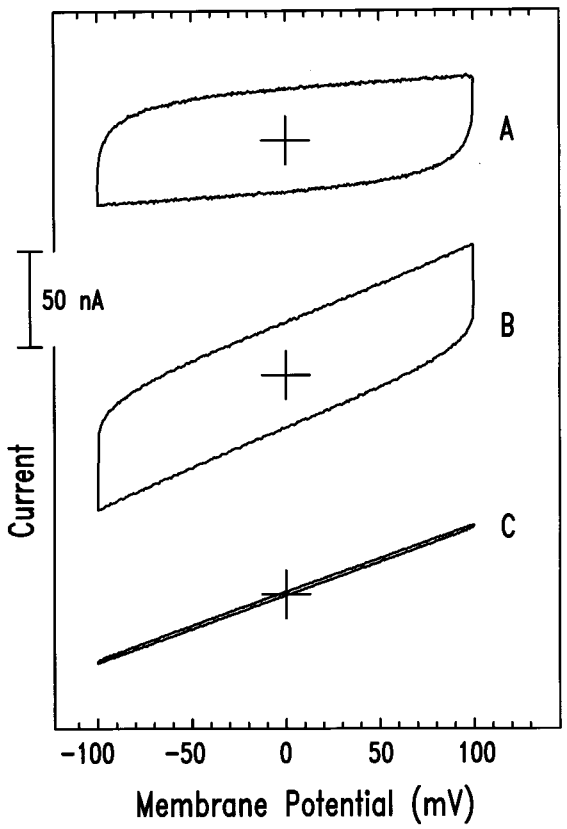

Figure 3. Cyclic voltammograms of an Au membrane clamped between two cells containing 0.1 M KCl and 0.2 mg/mL Triton X-100 (scan rate = 1 V/s): (A) without any pore (2×10^{-2} cm^2 Au exposed); (B) with a single pore (2×10^{-2} cm^2 Au exposed), and (C) with a single pore isolated by a photoresist mask (2×10^{-4} cm^2 Au exposed). The cross marks are the coordinate origins.

(26) Bard, A. J.; Faulkner, L. R. *Electrochemical Methods, Fundamentals and Applications*; Wiley: New York, 1980.

(27) DeBlois, R. W.; Bean, C. P. *Rev. Sci. Instrum.* **1970**, *41*, 909–916.

(28) The leakage pathway, for example, may be located along the grain boundaries of a polycrystalline Au film.

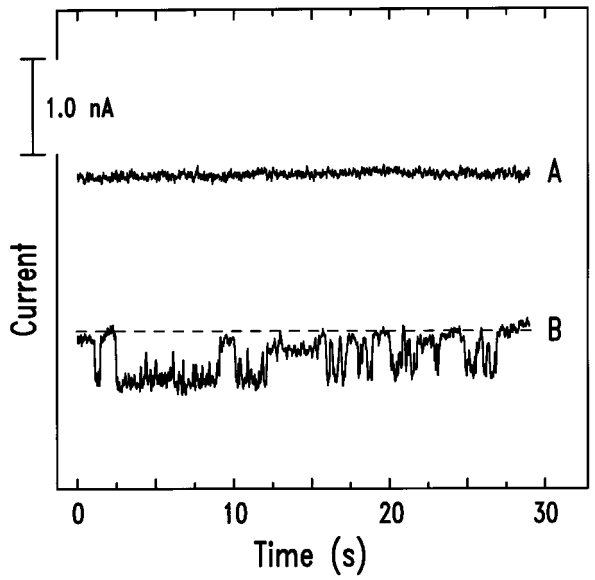

Figure 4. Transmembrane current as a function of time: (A) in the absence and (B) in the presence (only in the anode cell) of 440 nm diameter polystyrene spheres at a number density of 1.4×10^9 particles/mL. The single-pore membrane has essentially the same dimensions as the one for Figure 3C. The membrane was biased at a constant membrane potential of 200 mV, and the steady baseline current for both A and B (the dashed line for B) was 67 nA. Note that the negative-going current pulses (0.5 nA) are much smaller than the baseline current (67 nA). Thus, the zero current mark lies far outside the frame box of this figure.

minimized by masking the rest of the surface with a layer of photoresist (Figure 3C).

The ionic current across the pore varies linearly as a function of the membrane potential (Figure 3B,C). This property can be used to distinguish the ionic current from the CF current and to evaluate the geometric parameters of the pore. For example, the calculated pore length is 6.5 μm according to eq 2 with $\kappa = 1.29 \times 10^{-2}\ \Omega^{-1}\ \mathrm{cm}^{-1}$ for the 0.1 M KCl solution[29] and the measured d of 1.5 μm. This length agrees with the value (about 6 μm) measured directly from an optical micrograph of the membrane cross section. However, the pore length calculated from the thickness of electroplated Au is 8.0 μm, indicating a less-than-100% cathode efficiency or nonuniform electroplating.[30]

The single pore reported here can be used as a Coulter counter to detect polystyrene spheres (Figure 4). The quantized negative current pulses ranging from 0.3 to 6.5 s in width correspond to momentary reductions in pore conductance as single polystyrene spheres reside inside the pore. Thus, the pulse width is a direct measure of the transient residence time. The smallest pulse width detectable is limited by the *RC* time constant of the cell, where the *C* term is dominated by the double-layer capacitance of the membrane and the *R* is the uncompensated resistance resulting from the electrolyte located between the Ag/AgCl electrode and the membrane surface.[31] Clearly, minimizing the area of the bare metal surface not only reduces the CF current but also decreases the instrumental response time.

If the transport of the spheres is purely due to random diffusion, then the expected average transient time will be about 42 s,[32,33] much longer than the observed value. Thus, the spheres are driven by other gradient fields in addition to diffusion: most likely, via electrophoresis or electroosmosis. However, at present we do not have systematic data to resolve this issue. One of the experimental difficulties in transient measurements is the tendency of the pore being plugged, producing a transient trace without any pulse. This can be easily verified under an optical microscope: the light transmittance through a plugged pore is visibly reduced.

Extending the experimental protocol reported here to single pores of molecular dimensions will be very challenging. First, a template fiber having a diameter of a few nanometers is required. Carbon nanotubes are promising candidates,[34] but a mild and effective etching method for selectively removing the template nanotube needs to be identified. Second, manipulating a single nanotube is expected to be very difficult.[35] Finally, it is not known if a nanopore will be plugged easily as the mesopore shown in Figure 4. Chemical modification of the pore surface is one possible solution to this problem. In short, further reduction in pore size down to molecular dimensions depends on the availability of either advanced nanofabrication technology or simple methods of intrinsic merit that overcome the aforementioned challenges.

Summary and Conclusion

We have developed a template method for fabricating single-pore membranes. The method allows convenient control over the pore diameter and the pore length. We have also demonstrated that the single-pore membrane can be used as a Coulter counter to detect 440 nm diameter spherical particles. Single-pore Au membranes offer a convenient route for tailoring the surface chemistry of the pore with a SAM. However, Au membranes also show a drawback: the bare metal surface exposed to the electrolyte has to be minimized in order to decrease the interfering charging and faradaic current and to shorten the instrumental response time.

Acknowledgment. We gratefully acknowledge financial support from the National Science Foundation (CHE-9796203). Helpful discussions with Dr. Stephen W. Feldberg (Brookhaven National Laboratory) and Dr. Mark Spak (Hoechst Celanese) as well as technical assistance from Kevin Roberts (MTL)[21] are greatly appreciated.

LA980871A

(29) *CRC Handbook of Chemistry and Physics*, 70th ed.; Weast, R. C., et al., Eds.; CRC Press: Boca Raton, FL 1989; p D-169.

(30) Frederick, A. *Electroplating*; McGraw-Hill: New York, 1978.

(31) Do not confuse the uncompensated resistance (connected in series with the membrane capicitor) with the pore resistance (connected in parallel to the membrane capacitor).

(32) The equation, $t = l^2/D$, can be used to estimate the diffusional transient time, where l is the pore length (6.5 μm) and D (1×10^{-8} cm^2/s) is the diffusion coefficient estimated from the Stokes−Einstein equation.

(33) Kluijtmans, S. G. J. M.; Dhont, J. K. G.; Philipse, A. P. *Langmuir* **1997**, *13*, 4982−4987.

(34) Liu, J.; Rinzler, A. G.; Dai, H.; Hafner, J. H.; Bradley, R. K.; Boul, P. J.; Lu, A.; Iverson, T.; Shelimov, K.; Huffman, C. B.; Rodriguez-Macias, F.; Shon, Y.-S.; Lee, T. R.; Colbert, D. T.; Smalley, R. E. *Science* **1998**, *280*, 1253−1256.

(35) Wong, S. S.; Harper, J. D.; Lansbury, P. T., Jr.; Lieber, C. M. *J. Am. Chem. Soc.* **1998**, *120*, 603−604.